High-performance Microcavity Optical Sensor Connected with a Waveguide

Shuai Liu[1], **Zhiyuan Gu**[1], **Nan Zhang**[1], **Shumin Xiao**[2], **and Qinghai Song**[1,3]

[1]Department of Electrical and Information Engineering, Shenzhen Graduate School
Harbin Institute of Technology, Shenzhen 518055, China
[2]Department of Material Science and Engineering, Shenzhen Graduate School
Harbin Institute of Technology, Shenzhen 518055, China
[3]State Key Laboratory on Tunable Laser Technology, Institute of Opto-Electronics
Harbin Institute of Technology, Harbin 158015, China

Abstract— In this letter, we have numerically demonstrated a high-performance microcavity sensor which is connected with a waveguide directly. With input light and output light transmitting in the same waveguide, we propose a robust direct coupling mechanism of the microcavity. For a circular microcavity with a diameter of 4 µm and effective refractive index of 3.3, our numerical results show that the coupled modes are excited and more than 10^6 Q-factor is calculated from the transmission spectrum. Dramatically, the spectrum shows a Fano-shape resonance at specific wavelength. Using the Fano resonance, we detected a refractive index change on the order 10^{-5} and a nanoparticle with radius 5 nm. What's more, the sensor is insensitive to waveguide width and refractive index.

1. INTRODUCTION

Highly performed sensors have been an active research area for their widely applications in biological detection and environment monitoring. The early detection of viral particles responsible for human fatal diseases makes the prevention, diagnosis, and control possible. Though labelling detection method has made excellent achievements in this area, there are also problems with its detection mechanism. The labels may produce some other unknown signals and at some time the labels can be hardly conjugated with the target sample, which limits the experiment's scope. It is evident that there is a great need to label-free detection.

Whispering-gallery-mode (WGM) optical microcavities have been proposed as a prominent example to achieve high-precision detection in real-time and label-free manner, for their compact size, small mode volume, and ultrahigh Q factors ($Q \sim \omega t$, ω is the angular frequency and t is the lifetime) [1]. In the past two decades, high-Q whispering-gallery-mode resonators have shown remarkable detection limit and been used in various important applications, e.g., the detection of protein, DNA, single molecule [2–5] and so on. What's more, the modes can be excited in various geometries and materials, such as microsphere [6], cylinder [7], microring [8], and microtoroid [9] with refractive index ranging from 1.4 to 3.5. However, both of these sensors need a tapered-fiber to excite the high-Q WGMs by means of coupling light evanescently. This means the distance between the tapered-fiber and microcavity should be precisely controlled, usually less than a few hundred nanometers, and unfortunately the distance is sensitive to environmental disturbance.

2. DISCUSSION

In this letter, we report a new direct coupling mechanism to excite high-Q WGMs of the microcavity without using the tapered-fiber. By connecting a waveguide to microdisk directly, we show that the light can easily couple in the microcavity, excite the high-Q modes, and the corresponding detection signals couple out through the same in-put waveguide. In a small microcavity with 4-µm radius, our numerical results demonstrate detection of 10^{-5} refractive index change of the surrounding medium and single nanoparticle as small as 5 nm in radius. As the thicknesses are usually much smaller than their in-plane sizes, the microdisks are treated as two-dimensional objects by applying effective index of refraction n. The cavity studied here is schematically shown in Fig. 1(a). It is a circular cavity in radius R connected with a waveguide with width w. The emissions from such structure have been thoroughly studied in microlasers and unidirectional outputs along the waveguide are reported for the relative long-lived resonances. In principle, the unidirectional emissions and high output efficiencies do make sense. At the joint position, the TIR is totally broken. Thus the leakage along the waveguide is orders of magnitude larger than the evanescent tunneling and dominates the far field patterns.

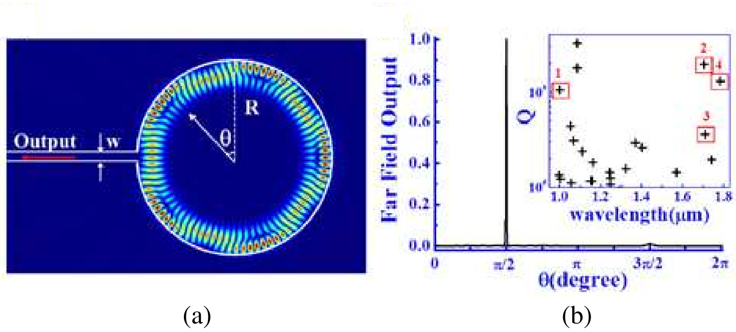

Figure 1: (a) The schematic picture of waveguide connected microdisk. $R = 4\,\mu m$, $w = 300\,nm$. (b) The normalized far-field output at wavelength 1703.39 nm with Q factor marked as 2 and electric field pattern in Fig. 1(a). The picture inset (b) is the calculated quality factors more than 2×10^5 at different wavelengths ranging from $1\,\mu m$ to $1.8\,\mu m$.

Figure 1(b) is an example of far field output pattern of the microdisk-waveguide systemand the corresponding electric field distribution is shown in Fig. 1(a) at wavelength 1703.39 nm. By exciting the high-Q modes in active devices, unidirectional outputs can be easily demonstrated. In consideration of time reversal symmetry, it is natural to think whether the high-Q modes can be efficiently excited with input light couples in through the waveguide. Below we will show that this conceive is actually true.

The microdisk-waveguide systems are numerically calculated with the Finite Element Method (Comsol Multiphsyics 3.5a). Here we set the effective refractive index $n = 3.3$ (GaAs) for transverse magnetic (TM, M is in plane) polarization and ignore the material dispersion. The microdisk with radius $R = 4\,\mu m$ and waveguide width $w = 0.3\,\mu m$ is surrounded by air ($n = 1$). Fig. 1(b) illustrates quality factors more than 10^5 of the microdisk-waveguide systems with wavelength ranging from $1\,\mu m$ to $1.8\,\mu m$. Both of these modes are simulated with Comsol 3.5a eigenvalue study. We take four relative high-Q modes (marked as red rectangle14) at wavelength 999.03 nm, 1703.40 nm, 1708.77 nm, and 1783.35 nm, respectively. To testify our conceive, we launch light at the waveguide around these mentioned resonance wavelengths. The light signals propagate along the waveguide and couple in the microdisk directly without using tapered-fiber. At the same time, we calculate the reflection spectrum taken at the plane marked as the dashed line in Fig. 2(e).

The normalized reflection spectrums shown in Figs. 2(a)–(d) are calculated by the reflective Poynting vector in the waveguide divided by total incident Poynting vector without the microdisk. From these spectrums, four peaks marked as red rectangle 1–4 can be easily found, which are 0.78, 0.91, 0.97, and 0.91, respectively. And the corresponding electric field patterns are shown in Fig. 2(e). The surprisingly high reflection efficiency means that almost all of the signals on resonance can easily couple out through the waveguide. In addition, the calculated Q ($Q \sim \lambda/\Delta\lambda$, λ is the resonance wavelength and $\Delta\lambda$ is the FWHM) factors are also very high, which are almost

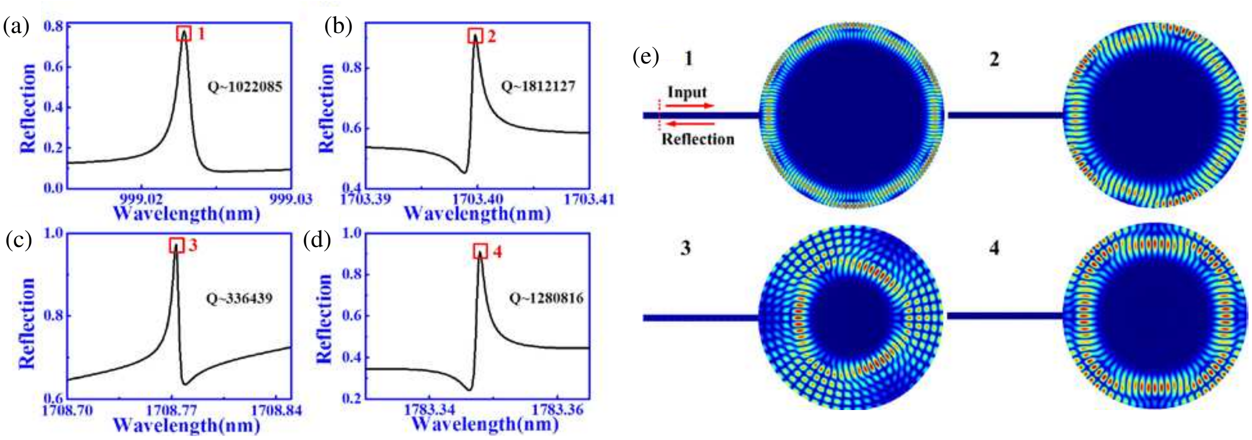

Figure 2: Calculated reflection spectra around 999.03 nm in (a), 1703.40 nm in (b), 1708.77 nm in (c), and 1783.35 nm in (d). (e) The electric field patterns of resonances marked as 1–4 in Figs. 2(a)–(d), respectively.

the same as the tapered-fiber coupling systems. So both of the resonance wavelengths, Q factors, and field patterns agree with the eigenvalue results in Fig. 1(b), demonstrating our assumption. This reveals that the direct coupling mechanism of microdisk-waveguide systems can easily excite the high Q modes as well as with high reflection efficiency, which is 'easy come, easy go'.

The formation of high Q resonances and high reflection efficiency can be understood as the following. Below,we will take the mode 2 with the highest Q factor in Fig. 2(b) for example. Once signals are coupled to the microdisk, three different leakages occur, which are the coupling to waveguide, refractive leakage, and the scattering at the junction of microdisk and waveguide. When the wavelength close to 1703.40 nm, it is easy to see that the coupled resonance (see Fig. 2(e) marked as 2) has a pentagon-shape field pattern and is confined along period-5 stable islands. As the pentagon-shape resonance is independent to the connecting waveguide, the waveguide thus will not affect the total internal reflection within stable islands directly,making the high Q factor realized. This is also why the leakage by refractive escape is orders of magnitude smaller than the coupling to waveguide. Therefore, more than 90% signals on resonance reflect along the connecting waveguide.

In additional to the high reflection efficiencies and high Q factors at many resonant wavelengths in Fig. 2, this surprising direct coupling mechanism is also robust to the waveguide with and refractive index of microdisk, which are essential for practical fabrications. The results are summarized in Fig. 3. We can see that the reflection is kept at a high value around 90% when the width of waveguide is changed from 0.1 μm to 0.5 μm (see Fig. 3(a)). Meanwhile, the high reflection efficiency ($> 90\%$) can also be obtained with a wide range of refractive index from $n = 2.7$ to $n = 3.5$ (Fig. 4(c)). The same as reflection efficiency, the microdisk-waveguide system with different waveguide width and refractive index also demonstrates relative high Q factors shown in Fig. 3(b) and Fig. 3(d), where all of them are more than 10^5. This means that the materials and their dispersions won't smear out the coupling mechanism.

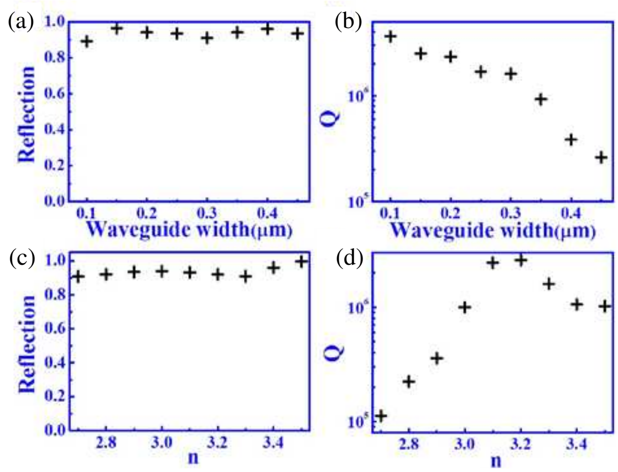

Figure 3: The maximum of reflection versus different waveguide width in (a) and refractive index in (c). (b) and (d) are the calculated quality factors versus different waveguide width and refractive index, respectively.

The resonant wavelengths of microcavity depend on the effective refractive index, which can be affected by, e.g., refractive index change of the surrounding medium and nanoparticle attached to its surface. Detection of such an effective index change can be made by either observing the shift of spectra or monitoring the change of light intensity from the output at a fixed wavelength. More interestingly, it is found that the lineshape in Fig. 2(b) is asymmetric Fano-shape resonance. The steep slope between minimum and maximal reflection makes the microdisk-waveguide system a natural highly sensitive sensor. Next, we will focus this reflection spectrum and test its detection properties.

Figure 4(a) shows the reflection spectrum of the sensor with different surrounding environment refractive indices from 1 to 1.0003 with step of 10^{-4}. The curves demonstrate an obvious red shift as the refractive index increases. Based on Fig. 4(a), the normalized reflective intensity variation at a fixed wavelength (1703.3998 nm) is plotted in Fig. 4(b) as a function of refractive index change Δn. We can see that a 10^{-5} change in refractive index can lead to almost 0.03 variation of reflective intensity. Such a high intensity variation means that Δn can be easily detected.

In addition, to test the properties of nanoparticle detection, we attach a single nanoparticle

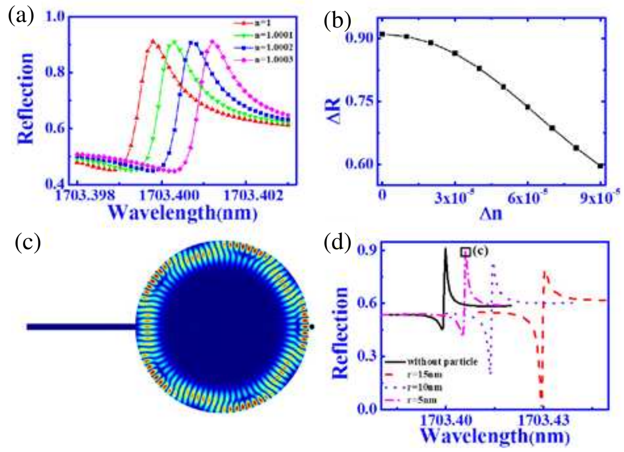

Figure 4: (a) Reflection spectra for different refractive indices n of the surrounding medium. (b) Reflection variation versus Δn at fixed wavelength of 1703.3998 nm. (c) Schematic picture of nanoparticle detection system. All the parameters are the same as Fig. 1(a). Single nanoparticle with refractive index $n_p = 3$ and radius r is attached to the microdisk at $\theta = 3/2\pi$. The electric field corresponds to the peak (marked as (c) in Fig. 4(d)) with $r = 5$ nm. (d) The calculated reflection spectra with different particle radius r.

with refractive index $n_p = 3$ to the microdisk. The schematic picture is shown in Fig. 4(c). All the parameters are the same as Fig. 1(a) except a nanoparticle is attached to the microdisk at $\theta = 3/2\pi$. Fig. 4(d) depicts the measured reflection spectrum with different particle radius r. For comparison, the black solid line in Fig. 4(d) is the reflection without nanoparticle. As a single particle in radius $r = 5$ nm is attached on the microdisk, the spectrum shows a red shift (the dash-dotted line) with both the maximal and minimal reflection decrease. And this trend keeps as the particle radius increases, demonstrating the effective nanoparticle size sensing.

3. CONCLUSION

We have demonstrated a direct coupling optical sensor which is robust to waveguide width and refractive index. Our numerical results show that light can be either easily coupled in the microcavity or easily coupled out through the same waveguide. Refractive index change on the order 10^{-5} and single nanoparticle with radius 5nm can be detected with this sensor.

REFERENCES

1. Vahala, K. J., "Optical microcavities," *Nature*, Vol. 424, 839–846, 2003.
2. Vollmer, F. and S. Arnold, "Whispering-gallery-mode biosensing: Label-free detection down to single molecules," *Nature Methods*, Vol. 5, No. 7, 591–596, 2008.
3. Vollmer, F., D. Braun, A. Libchaber, et al., "Protein detection by optical shift of a resonant microcavity," *Applied Physics Letters*, Vol. 80, No. 21, 4057–4059, 2002.
4. Arnold, S., M. Khoshsima, I. Teraoka, et al., "Shift of whispering-gallery modes in microspheres by protein adsorption," *Optics Letters*, Vol. 28, No. 4, 272–274, 2003.
5. Vollmer, F. and L. Yang, "Review Label-free detection with high-Q microcavities: A review of biosensing mechanisms for integrated devices," *Nanophotonics*, Vol. 1, Nos. 3–4, 267–291, 2012.
6. Cai, M., O. Painter, and K. J. Vahala, "Observation of critical coupling in a fiber taper to a silica-microsphere whispering-gallery mode system," *Phys. Rev. Lett.*, Vol. 85, 74, 2000.
7. Li, H. and X. Fan, "Characterization of sensing capability of optofluidic ring resonator biosensors," *Applied Physics Letters*, Vol. 97, No. 1, 011105, 2010.
8. Yalcin, A., K. C. Popat, J. C. Aldridge, et al., "Optical sensing of biomolecules using microring resonators," *IEEE Journal of Selected Topics in Quantum Electronics*, Vol. 12, No. 1, 148–155, 2006.
9. Monifi, F., Ş. K. Özdemir, and L. Yang, "Tunable add-drop filter using an active whispering gallery mode microcavity," *Applied Physics Letters*, Vol. 103, No. 18, 181103, 2013.